Published in final edited form as:

Oncogene. 2015 June ; 34(26): 3369–3376. doi:10.1038/onc.2014.285.

Autophagy regulates tissue overgrowth in a context-dependent manner

Ernesto Pérez[1,2], **Gautam Das**[1,2], **Andreas Bergmann**[1], and **Eric H. Baehrecke**[1]

[1]Department of Cancer Biology, University of Massachusetts Medical School, Worcester, MA, USA

Abstract

Autophagy is a catabolic process that has been implicated as both a tumor suppressor and in tumor progression. Here, we investigate this dichotomy in cancer biology by studying the influence of altered autophagy in *Drosophila* models of tissue overgrowth. We find that the impact of altered autophagy depends on both genotype and cell type. As previously observed in mammals, decreased autophagy suppresses Ras-induced eye epithelial overgrowth. By contrast, autophagy restricts epithelial overgrowth in a Notch-dependent eye model. Even though decreased autophagy did not influence Hippo pathway-triggered overgrowth, activation of autophagy strongly suppresses this eye epithelial overgrowth. Surprisingly, activation of autophagy enhanced Hippo pathway-driven overgrowth in glia cells. These results indicate that autophagy has different influences on tissue growth in distinct contexts, and highlight the importance of understanding the influence of autophagy on growth to augment a rationale therapeutic strategy.

Keywords

autophagy; epithelial growth; glia; cancer; *Drosophila*

Introduction

Autophagy is used to deliver cytoplasmic material to lysosomes for degradation. Autophagy is activated by multiple forms of stress, including reduced nutrient and oxygen levels, elevated reactive oxygen species, and organelle damage, many of which have been implicated in tumor formation and progression (1). During autophagy, cargoes such as damaged organelles and protein aggregates are recruited into double membrane autophagosome vesicles for clearance by fusion with lysosomes to form autolysosomes where they are degraded by hydrolases (2). Thus, autophagy serves to alleviate stress, and failure to do so could promote genetic alterations and tumor development (3, 4). Although much is known about how autophagy (*Atg*) genes control this process based on studies in

Correspondence: A. Bergmann and E.H. Baehrecke, Department of Cancer Biology, University of Massachusetts Medical School, 364 Plantation Street, Worcester, MA, 01505, USA. Andreas.Bergmann@umassmed.edu; Eric.Baehrecke@umassmed.edu.
[2]These authors contributed equally to this work.

Conflict of Interest: The authors declare no conflict of interest.

yeast, our understanding of the multiple potential roles of autophagy in animal cell, tissue and tumor biology remains rudimentary.

Autophagy has been implicated as both a tumor suppressor and in tumor progression (5). This paradox may be explained by multiple possibilities, including inherent differences in the cells and tissues where tumors arise, the presence of secondary genetic alterations in tumor promoting genes, and numerous others. For example, recent studies indicate that p53 status influences the impact of autophagy on K-Ras-triggered mouse models of pancreatic and lung cancers; loss of *Atg* gene function inhibits tumor progression in the presence of p53, but in the absence of p53 loss of autophagy accelerates tumor onset (6, 7). In addition, much of what is known about the influence of autophagy on tumor biology is based on studies of the *Beclin1/Atg6* gene, and it is now clear that this gene influences a wide variety of vesicle trafficking processes, including endocytosis, protein secretion and autophagy (8, 9). Furthermore, while the role of autophagy in oncogenic Ras-driven tumor growth and the dependence on p53 status has been investigated, the influence of autophagy in different tumor contexts is largely unknown. Thus, studies of the role of autophagy in other tumor models are needed.

The fruit fly *Drosophila melanogaster* serves as a useful model to study epithelial growth, and the influence of oncogenes and tumor suppressors on epithelial overgrowth. Mammalian oncogenes and tumor suppressors are conserved in *Drosophila* and their deregulation can cause tissue overgrowth (10, 11). For example, oncogenic Ras which is associated with approximately 30% of human tumors (12), triggers epithelial overgrowth and also inhibits apoptosis in *Drosophila* (13-15). De-regulation of Notch causes certain forms of cancer in humans (16), and is also associated with severe overgrowth in *Drosophila*. One striking example of Notch-induced overgrowth is the *eyeful* phenotype which is characterized by strong eye overgrowth and secondary metastasis-like growths (17). Another growth regulatory pathway which is deregulated in human cancer is the Hippo pathway which was originally discovered in *Drosophila* (18). Critical components in the Hippo pathway include the Hippo and Warts kinases which prevent the transcriptional co-activator Yorkie (YAP in mammals) from translocating to the nucleus to induce cell proliferation. In addition, mutations in the tumor suppressor *scribble* (*scrib*) cause loss of apical-basal polarity, failure to differentiate and apoptosis that involves c-Jun N-terminal kinase (JNK)-induced signaling (19). However, if *scrib* mutant cell clones are protected from apoptosis by expression of transgenes encoding either dominant negative *JNK* (JNK^{DN}), the caspase inhibitor p35 or the oncogene Ras^{V12} (referred to as *scrib+*JNK^{DN}, *scrib+P35* or *scrib+*Ras^{V12}), *scrib* mutant cells survive and unleash their full oncogenic activity, resulting in over-proliferation and formation of neoplastic tissue masses (20-22).

The influence of autophagy on tissue overgrowth caused by most of these growth regulatory factors is unknown. Here, we investigate the influence of altered autophagy on tissue overgrowth in *Drosophila*. We discover that the influence of loss and gain of autophagy differs depending on the growth-inducing stimulus and tissue. Like in mammals, autophagy is required for Ras-triggered epithelial overgrowth. In contrast, autophagy restricts increased epithelial growth in the Notch-dependent *eyeful* overgrowth model. Furthermore, increased growth driven by either loss of the growth regulator *hippo* or mis-expression of Yorkie is not

influenced by decreased *Atg* gene function. Nevertheless, ectopic autophagy strongly suppresses epithelial overgrowth in these models. In contrast, activation of autophagy enhanced Yorkie-driven overgrowth in glia cells. These studies highlight the potential complexities of modulating autophagy in different *in vivo* models of cell and tissue overgrowth, and encourage a greater understanding of the influence of modulating autophagy for therapeutic purposes.

Results

Autophagy can enhance or suppress tissue growth depending on genotype

Studies in mammalian Ras-driven cancer models indicate that autophagy is required for tumor progression (6, 7, 23). As previously described, expression of activated Ras^{V12} combined with loss of *scrib* in the *Drosophila* eye epithelium results in a strong tissue overgrowth phenotype (note the increase in GFP-expressing mutant tissue) compared to equivalent wild type tissue (Figure 1a,a′,b,b′) (20, 22). We analyzed the effect of reduced autophagy on *scrib+*Ras^{V12}-driven overgrowth by expression of RNAi against *Atg1* ($Atg1^{IR}$). Similar to mammalian K-Ras-driven models of cancer, $Atg1^{IR}$ suppresses either *scrib+*Ras^{V12}- or Ras^{V12}-driven overgrowth (Figure 1c,c′ and Supplementary Figure 1b,c, note the reduction in GFP-expressing mutant tissue), indicating that autophagy is required for tissue overgrowth.

Ras^{V12} not only protects cells from apoptosis, but also has other oncogenic effects that drive tumor growth. To uncouple these different effects of Ras^{V12} with respect to autophagy, we blocked apoptosis by expression of either JNK^{DN} or p35, but did not induce any other oncogenic activity. As reported previously (20), inhibition of apoptosis is sufficient to trigger *scrib*-induced overgrowth in epithelial tissue (Figure 1d,e,f,g, note the increase in GFP-expressing mutant tissue compared to control). Surprisingly, in contrast to *scrib +*Ras^{V12}, in *scrib* mutants with impaired apoptosis by expression of either JNK^{DN} or p35, reduction of autophagy using the same *Atg1* RNAi transgene as in Figure 1c enhances *scrib*-induced overgrowth (Figure 1h, i, note the increase in GFP-expressing mutant tissue compared to tissue lacking GFP). Most strikingly, autophagy-deficient *scrib+*JNK^{DN} cells make up almost the entire eye tissue (Figure 1h) suggesting that autophagy restricts growth of apoptosis-inhibited *scrib* cell clones. Similarly, reduction of autophagy in apoptotic *scrib* mutant cells slightly increases clone size (Supplementary Figure 1d,e). These results indicate that oncogenic Ras^{V12} requires autophagy to drive strong tissue overgrowth; in the presence of Ras^{V12}, autophagy promotes growth of *scrib* mutant tissue (Figure 1c), and in the absence of Ras^{V12}, autophagy restricts tissue growth (Figure 1h, i). These observations are consistent with data from mammalian tumor models and encourage further characterization of the role of autophagy in other oncogenic and cellular contexts in *Drosophila*.

Autophagy suppresses *eyeful*-induced tissue overgrowth

To examine the role of autophagy in a different oncogenic fly model, we used the established tissue overgrowth model called *eyeful*. *eyeful* is a Notch-dependent overgrowth model resulting from mis-expression of the Notch ligand *Delta* and of two chromatin modifiers, *lola* and *pipsqueak*, in the eye (17). The *eyeful* phenotype consists of eye tissue

overgrowth that ranges from mild overgrowth to overgrowth with tissue folds (Figure 2a,b,f,g) as well as less frequent secondary ”metastasis-like” eye growths in other parts of the body (17). The *eyeful*-induced overgrowth is visible in developing larval antennal-eye precursor tissues, called imaginal discs (Figure 2l,m). To examine a potential contribution of autophagy to the *eyeful* phenotype, we decreased the function of 12 different *Atg* genes (*Atg1, Atg6, Atg12, Atg5, Atg7, Atg4a, Atg4b, Atg8a, Atg8b, Atg3, Atg9, Atg18*) by RNAi. Strikingly, knock-down of any of these *Atg* genes strongly enhances *eyeful*-induced tissue overgrowth in both the adult eye (compare Figure 2c,d,e to 2b; summarized in Figure 2j) and in imaginal discs (compare Figure 2n,o to 2m), but do not influence development of wild-type eye tissue (Supplementary Figure 2). Even more strikingly, these eyes do not only display enhanced overgrowth, but often grow out from the eye in the form of projections (Figure 2h,i; arrows). Knock-down of the 12 *Atg* genes in the *eyeful* overgrowth model resulted in significant increases in the percentage of animals with eye projections (Figure 2k). *eyeful* imaginal disc cells also possessed increased mCherry-Atg8 autophagy reporter puncta (compare Supplementary Figure 3d' to b') and accumulate Ref(2)P proteins (*Drosophila* ortholog of p62 and autophagy substrate) in areas where mCherry-Atg8 labeling is either low or absent (compare Supplementary Figure 3d” to b”). These data indicate that in the context of oncogenic Notch signaling, autophagy restricts growth. This is in strong contrast to the influence of autophagy as an enhancer of Ras^{V12}-driven overgrowth (Figure 1c). These observations indicate that autophagy differentially influences tissue growth depending on the oncogenic activity in a given epithelium.

To further characterize the function of autophagy in tissue growth, we tested the effect of increased autophagy on the *eyeful* model. Expression of Atg1 is sufficient to induce autophagy in multiple *Drosophila* cell and tissue types (24-26). Consistent with our loss-of-*Atg* gene function data, induction of autophagy by expression of Atg1 strongly suppresses *eyeful*-induced tissue overgrowth (Figure 3a,b). We next addressed if suppression of *eyeful* tissue overgrowth by Atg1 expression depends on *Atg* gene function. To accomplish this task, we co-expressed Atg1 with RNAi transgenes targeting either *Atg8* ($Atg8^{IR}$) or *Atg12* ($Atg12^{IR}$) in *eyeful* animals and examined eye tissue overgrowth. Expression of either $Atg8^{IR}$ or $Atg12^{IR}$ reverts the Atg1-induced suppression of the *eyeful* overgrowth back to overgrown eye tissue (Figure 3c, d) indicating that suppression of *eyeful* overgrowth by Atg1 expression is dependent on the autophagy pathway. Taken together, these results indicate that ectopically induced autophagy functions as a suppressor of *eyeful*-induced tissue overgrowth.

Atg1-induced autophagy can induce either caspase-dependent or -independent cell death (24, 25). Therefore, we assessed the role of caspases in the suppression of *eyeful*-induced overgrowth by Atg1 expression. To assay apoptotic cell death, we immuno-labeled larval antennal-eye disc tissues with antibodies to detect cleaved caspase-3. Interestingly, we observed cleaved caspases in *eyeful* larval eye discs alone (Figure 3e) suggesting that *eyeful* induces apoptosis that is associated with overgrowth. Although Atg1 expression in *eyeful* tissue is also associated with elevated cleaved caspase-3 labeling (Figure 3f), it is unclear if it is increased over *eyeful* alone (Figure 3e). Importantly, cleaved caspase-3 labeling was observed when either $Atg8^{IR}$ or $Atg12^{IR}$ were co-expressed with Atg1 in *eyeful* tissue

(Figure 3g,h). Combined, these results suggest that cleaved caspase-3 labeling is associated with *eyeful*-induced tissue overgrowth, but does not appear to be associated with Atg1-triggered autophagy.

Our data suggest that apoptosis does not play a significant role in *Atg1*-dependent suppression of *eyeful*-induced tissue overgrowth. Nevertheless, because we observed cleaved caspase-3 in *eyeful* tissue (Figure 3e), we explored the role of caspases for *eyeful*-induced tissue overgrowth by expressing the caspase inhibitor *p35* in *eyeful* tissue. This treatment strongly enhances tissue overgrowth (Figure 3k) compared to *eyeful* alone (Figure 3j). In addition, decreased *Atg7* function further enhanced the *eyeful* and *p35* overgrowth phenotype (Figure 3k,l). Combined, these data suggest that both caspases and autophagy restrict tissue growth in the *eyeful* model.

Ectopic autophagy suppresses or enhances *hippo* pathway-induced overgrowth depending on tissue

The evolutionarily conserved Hippo signaling pathway is important for proper growth control and tumorigenesis. *hippo* is a tumor suppressor, as loss of *hippo* causes tissue overgrowth (Figure 4a,b, e,f) (18). We reduced autophagy by expression of $Atg8^{IR}$ in $hippo^{-}$ mutant cells. However, this treatment had little effect on either mutant cell clone or tissue size in imaginal discs and in adult heads (Figure 4c,g). By contrast, induction of autophagy by mis-expression of Atg1 in $hippo^{-}$ mutant cell clones dramatically reduces mutant clone size in larval imaginal eye tissue and adult eyes (Figure 4d,h). Thus, while endogenous autophagy does not restrict $hippo^{-}$-induced tissue overgrowth, the induction of autophagy strongly suppresses $hippo^{-}$ induced tissue overgrowth. Similarly, mis-expression of the Hippo pathway transcription factor Yorkie in the eye causes strong eye overgrowth which is suppressed by simultaneous overexpression of Atg1 (Figure 4i-l). Analyses of imaginal discs showed that expression of Atg1 decreases Yorkie-induced cell proliferation based on phospo-histone H3 (PH3) antibody staining (Supplementary Figure 4).

Our data indicate that modulation of autophagy has distinct impacts on eye epithelial growth depending on the genetic alteration that drives overgrowth. Since modulation of autophagy in *hippo* mutant cells had a modest influence on eye tissue growth, we tested if altered autophagy has an impact on growth of a different cell type, glia cells, undergoing Yorkie-induced overgrowth (27). In addition, we examined the role of autophagy in Yorkie-induced glia overgrowth in a different tissue, the leg imaginal discs. Expression of Yorkie in glia cells of the leg imaginal discs strongly increases the number of glia cells using Repo antibody as glia cell marker (Figure 5b,b'). Ectopic induction of Atg1 slightly increases the number of repo-positive glia cells in leg discs (Figure 5c,c'). Surprisingly, however, expression of Atg1 dramatically enhances Yorkie-induced glia overgrowth in larval leg discs (Figure 5d,d'). A similar, although somewhat weaker effect of Atg1-induced autophagy was observed in Yorkie-induced glia overgrowth in eye imaginal discs (Supplementary Figure 5). These observations are surprising as ectopic Atg1 expression acts as a strong suppressor of overgrowth in epithelial tissue (Figure 3b, 4d), including *hippo*-induced overgrowth. Thus, while ectopic autophagy suppresses *hippo*-induced overgrowth in epithelial tissue, it enhances growth in a population of glia cells.

Discussion

Substantial evidence indicates that autophagy can play distinct roles in different cellular contexts. In cancer, autophagy has been implicated in both tumor suppression and tumor progression (5). Studies in mice indicate that autophagy restricts tumor initiation by restricting genome damage (3, 4). By contrast, autophagy appears to promote tumor progression once tumors are established by enabling cancer cell survival (23, 28). However, no previous study has systematically analyzed the influence of autophagy when either distinct oncogenic stimuli are activated within a single epithelial tissue, or if an identical oncogenic stimulus is activated in different cellular contexts.

Here we investigate the influence of autophagy in distinct epithelial cell contexts in *Drosophila*. We find that, like in mammals, autophagy promotes overgrowth in the context of a Ras-driven eye epithelial model. By contrast, autophagy suppresses overgrowth in the same epithelial tissue in a model with altered JNK function. Strikingly, autophagy also suppresses severe overgrowth observed in the eyes of a model involving Notch activation. Finally, we show that autophagy fails to suppress overgrowth in the eye epithelium when Hippo function is reduced, and that activation of autophagy enhances overgrowth in glia. Therefore, our results indicate a wide variety of potential influences of autophagy on cell and tissue growth, and that these may depend on both oncogenic signal and cell type.

Autophagy is a catabolic process that is activated to alleviate cell stress, and also maintains bioenergetic homeostasis under nutrient restriction. In both of these scenarios, autophagy promotes cell survival. Therefore, it is possible that the different influences of autophagy on tissue growth are related to these different survival-associated functions and the influence of either different growth or oncogenic signals on the pathways influenced by autophagy. For example, metabolism is known to be altered in many cancers (29), and since autophagy is a catabolic process this may explain one type of cellular outcome. Alternatively, stress activates autophagy, and altered metabolism combined with a different ability to cope with stress because of altered signaling could result in a different cell and tissue outcome. Autophagy has also been implicated in cell death, and how autophagy promotes cell death also appears context dependent (30). Therefore, many possibilities exist for how autophagy may contribute to epithelial growth.

Multiple oncogenic and growth regulatory signals have been shown to influence autophagy, and autophagy influences growth pathways. For example, mTOR directly represses autophagy by phosphorylation of Atg13, and factors upstream of mTOR, including p110, PTEN and Akt, have been shown to influence autophagy (31). In addition, autophagy influences mTOR activity under nutrient restriction by the association of this kinase with autolysosomes that control nutrient availability and the activity of mTOR (32, 33). In addition, both the Ras and Hippo pathways influence autophagy (25, 34). Interestingly, activated Ras often represses autophagy, but in at least some tumor cell lines with activated Ras autophagy is activated (35). These studies further emphasize the important relationship between nutrient sensing, growth regulatory and autophagy pathways.

The modulation of autophagy is considered to be a promising therapeutic strategy for treating cancer. Our studies highlight the importance of considering tumor genotype when autophagy is targeted for therapies. Therefore, much work is needed to better understand the potential impact of altered autophagy in different cancers. At this stage, it is unclear which tumor characteristics are best to consider when manipulating autophagy for therapeutic purposes. Our data indicating that decreased autophagy suppresses Ras-triggered overgrowth is consistent with work in mammals, but recent studies indicate that p53 status is important to consider when treating Ras-driven tumors (6, 7). Future studies should enable us to classify tumors such that modulation of autophagy is a rationale therapeutic strategy.

Materials and Methods

Fly stocks, over-expression and clonal analysis, and quantification of overgrowth

All crosses were kept at 25°C, except where indicated. Either Canton-S or w^{1118} was used as control. For induction of tissue overgrowth *eyeful/Cyo* (*eyeless-Gal4>UAS-delta, GS88A8 UAS-lola, UAS-pipsqueak*)(17), *eyeless-Gal4, gmr-Gal4, UAS-yorkie* (36), UAS- Ras^{V12}, *UAS-dicer2; repo-Gal4 UAS-MCD::GFP/TM6B* (27), *yw hs-FLP; sp/Cyo; FRT82B* $scrib^{2}$*/ TM3, w; UAS-p35; FRT82B* $scrib^{2}$*/TM6B, UAS-bsk*^{DN}*; sp/Cyo; FRT82B* $scrib^{2}$*/TM6B, yw; UAS-*Ras^{V12}*FRT82B* $scrib^{2}$*/TM6B* (37), *w; FRT42D* $hippo^{3D}$*/Cyo* were used. For down-regulation or induction of autophagy we used lines from Vienna Drosophila RNAi Center (VDRC) and Bloomington (BL) Stock Center unless noted: $Atg1^{IR}$ VDRC Transformant ID (TID) 16133, $Atg6^{IR}$ TID 11647, $Atg12^{IR}$ BL34675, $Atg5^{IR}$ BL27551, $Atg4b^{IR}$ TID 11855, $Atg4a^{IR}$ TID 11315, $Atg8a^{IR}$ TID 43097, $Atg8b^{IR}$ TID 17079, $Atg3^{IR}$ TID 108666, $Atg9^{IR}$ TID 2029, $Atg7^{IR}$ TID 45561, $Atg18^{IR}$ TID 22646, $Atg1^{K38Q}$, $Atg1^{6B}$, and $Atg1^{GS10797}$ (24, 25). To induce cell clones *yw ey-FLP1; Act>y+>Gal4 UAS-GFP*^{S65T}*; FRT82B tubGal80* and *yw ey-FLP; FRT42D tubulin-Gal80; tub-Gal4 UAS-CD8-GFP/T(2;3)SM5-TM6B* were used. For mCherry-Atg8 analysis, we used *UAS-mCherry-Atg8* (38).

The UAS-Gal4 system was used to mis-express genes of interest or express RNAi against target genes (39). MARCM (mosaic analysis with a repressible cell marker) was used to express genes of interest or express RNAi against target genes in mutant clones (40).

For larval staging egg-laying was allowed for 24 hours, and larvae were aged at 25 °C. Wandering 3rd instar wild-type larvae were collected and dissected on day 5. On day 12 wandering 3rd instar larvae with either *UAS-*Ras^{V12} $scrib^{2}$ or *UAS-*$Atg1^{IR}$ *UAS-*Ras^{V12} $scrib^{2}$ MARCM clones were collected and dissected.

GraphPad Prism 6 software was used to quantify animals with overgrown eyes, secondary growths, or eye projections. Adult eye or head capsule images were taken with a Zeiss SteReo Discovery.V20 stereo microscope and processed with Zen 2012 blue edition imaging software.

Immunostaining and Microscopy

Eye-antennal or leg imaginal discs from wandering 3rd instar larvae or white prepupa were dissected and stained with the following antibodies: rabbit anti-cleaved caspase-3 (1:200, Cell Signaling Technology, 9661), rabbit anti-Ref(2)P (1:2000, G. Juhasz) (41), rabbit anti-

PH3 (1:1000, Upstate), rat anti-ELAV (1:40, Developmental Studies Hybridoma Bank, 7E8A10) and mouse anti-repo (1:20, Developmental Studies Hybridoma Bank, 8D12). FITC, Cy-3 and Cy-5 fluorescently-conjugated secondary antibodies were from Jackson ImmunoResearch. Vectashield mounting medium with DAPI was from Vector Laboratories. Images were obtained with a Zeiss LSM 700 confocal microscope with Zen 2012 imaging software and processed with Adobe Photoshop CS5.1.

Quantification and Statistical Analysis

PH3-positive cells were counted posterior to the morphogenetic furrow. Ten representative eye discs were counted for each genotype. GraphPad Prism 6 software was used to determine the average number of mitotic cells per eye disc, and a *P* value was obtained using a two-tailed *t*-test. All quantitative data are shown as mean ± s.d.

Supplementary Material

Refer to Web version on PubMed Central for supplementary material.

Acknowledgments

We thank T. Chang, M. Dominguez, M. Freeman, G. Halder, G. Juhasz, M. Kango-Singh, T.P. Neufeld, the Bloomington Stock Center, the VDRC for flies and antibodies, J. Lindblad, C. Nelson, and T. Fortier for technical support, and the Bergmann and Baehrecke labs for constructive comments. This work was supported by NIH grants GM068016 to AB and CA159314 to EHB. EHB is an Ellison Medical Foundation Scholar.

References

1. Kondo Y, Kanzawa T, Sawaya R, Kondo S. The role of autophagy in cancer development and response to therapy. Nat Rev Cancer. 2005; 5:726–34. [PubMed: 16148885]
2. Mizushima N, Komatsu M. Autophagy: Renovation of Cells and Tissues. Cell. 2011; 147:728–41. [PubMed: 22078875]
3. Mathew R, Kongara S, Beaudoin B, Karp CM, Bray K, Degenhardt K, et al. Autophagy suppresses tumor progression by limiting chromosomal instability. Genes Dev. 2007; 21:1367–81. [PubMed: 17510285]
4. Karantza-Wadsworth V, Patel S, Kravchuk O, Chen G, Mathew R, Jin S, et al. Autophagy mitigates metabolic stress and genome damage in mammary tumorigenesis. Genes Dev. 2007; 21:1621–35. [PubMed: 17606641]
5. Mathew R, Karantza-Wadsworth V, White E. Role of autophagy in cancer. Nat Rev Cancer. 2007; 7:961–7. [PubMed: 17972889]
6. Rosenfeldt MT, O'Prey J, Morton JP, Nixon C, MacKay G, Mrowinska A, et al. p53 status determines the role of autophagy in pancreatic tumour development. Nature. 2013; 504:296–300. [PubMed: 24305049]
7. Rao S, Tortola L, Perlot T, Wirnsberger G, Novatchkova M, Nitsch R, et al. A dual role for autophagy in a murine model of lung cancer. Nat Commun. 2014; 5:3056. [PubMed: 24445999]
8. Funderburk SF, Wang QJ, Yue Z. The Beclin 1-VPS34 complex--at the crossroads of autophagy and beyond. Trends Cell Biol. 2010; 20:355–62. [PubMed: 20356743]
9. Shravage BV, Hill JH, Powers CM, Wu L, Baehrecke EH. Atg6 is required for multiple vesicle trafficking pathways and hematopoiesis in Drosophila. Development. 2013; 140:1321–9. [PubMed: 23406899]
10. Tipping M, Perrimon N. Drosophila as a model for context-dependent tumorigenesis. J Cell Physiol. 2014; 229:27–33. [PubMed: 23836429]

11. Rudrapatna VA, Cagan RL, Das TK. Drosophila cancer models. Dev Dyn. 2012; 241:107–18. [PubMed: 22038952]
12. Bos JL. ras oncogenes in human cancer: a review. Cancer Res. 1989; 49:4682–9. [PubMed: 2547513]
13. Karim FD, Rubin GM. Ectopic expression of activated Ras1 induces hyperplastic growth and increased cell death in Drosophila imaginal tissues. Development. 1998; 125:1–9. [PubMed: 9389658]
14. Bergmann A, Agapite J, McCall K, Steller H. The Drosophila gene hid is a direct molecular target of Ras-dependent survival signaling. Cell. 1998; 95:331–41. [PubMed: 9814704]
15. Kurada P, White K. Ras promotes cell survival in Drosophila by downregulating hid expression. Cell. 1998; 95:319–29. [PubMed: 9814703]
16. Lobry C, Oh P, Aifantis I. Oncogenic and tumor suppressor functions of Notch in cancer: it's NOTCH what you think. J Exp Med. 2011; 208:1931–5. [PubMed: 21948802]
17. Ferres-Marco D, Gutierrez-Garcia I, Vallejo DM, Bolivar J, Gutierrez-Aviño FJ, Dominguez M. Epigenetic silencers and Notch collaborate to promote malignant tumours by Rb silencing. Nature. 2006; 439:430–6. [PubMed: 16437107]
18. Johnson R, Halder G. The two faces of Hippo: targeting the Hippo pathway for regenerative medicine and cancer treatment. Nat Rev Drug Discov. 2014; 13:63–79. [PubMed: 24336504]
19. Elsum I, Yates L, Humbert PO, Richardson HE. The Scribble-Dlg-Lgl polarity module in development and cancer: from flies to man. Essays Biochem. 2012; 53:141–68. [PubMed: 22928514]
20. Pagliarini RA, Xu T. A genetic screen in Drosophila for metastatic behavior. Science. 2003; 302:1227–31. [PubMed: 14551319]
21. Igaki T, Pagliarini RA, Xu T. Loss of cell polarity drives tumor growth and invasion through JNK activation in Drosophila. Curr Biol. 2006; 16:1139–46. [PubMed: 16753569]
22. Brumby AM, Richardson HE. scribble mutants cooperate with oncogenic Ras or Notch to cause neoplastic overgrowth in Drosophila. EMBO J. 2003; 22:5769–79. [PubMed: 14592975]
23. Guo JY, Karsli-Uzunbas G, Mathew R, Aisner SC, Kamphorst JJ, Strohecker AM, et al. Autophagy suppresses progression of K-ras-induced lung tumors to oncocytomas and maintains lipid homeostasis. Genes Dev. 2013; 27:1447–61. [PubMed: 23824538]
24. Scott RC, Juhász G, Neufeld TP. Direct induction of autophagy by Atg1 inhibits cell growth and induces apoptotic cell death. Curr Biol. 2007; 17:1–11. [PubMed: 17208179]
25. Berry DL, Baehrecke EH. Growth arrest and autophagy are required for salivary gland cell degradation in *Drosophila*. Cell. 2007; 131:1137–48. [PubMed: 18083103]
26. Chang TK, Shravage BV, Hayes SD, Powers CM, Simin RT, Harper JW, et al. Uba1 functions in Atg7- and Atg3-independent autophagy. Nat Cell Biol. 2013; 15:1067–78. [PubMed: 23873149]
27. Reddy BV, Irvine KD. Regulation of Drosophila glial cell proliferation by Merlin-Hippo signaling. Development. 2011; 138:5201–12. [PubMed: 22069188]
28. Takamura A, Komatsu M, Hara T, Sakamoto A, Kishi C, Waguri S, et al. Autophagy-deficient mice develop multiple liver tumors. Genes Dev. 2011; 25:795–800. [PubMed: 21498569]
29. Vander Heiden MG, Cantley LC, Thompson CB. Understanding the Warburg effect: the metabolic requirements of cell proliferation. Science. 2009; 324:1029–33. [PubMed: 19460998]
30. McPhee CK, Baehrecke EH. Autophagy in Drosophila melanogaster. Biochim Biophys Acta. 2009; 1793:1452–60. [PubMed: 19264097]
31. Scott RC, Schuldiner O, Neufeld TP. Role and regulation of starvation-induced autophagy in the Drosophila fat body. Dev Cell. 2004; 7:167–78. [PubMed: 15296714]
32. Yu L, McPhee CK, Zheng L, Mardones GA, Rong Y, Peng J, et al. Autophagy termination and lysosome reformation regulated by mTOR. Nature. 2010; 465:942–6. [PubMed: 20526321]
33. Sancak Y, Bar-Peled L, Zoncu R, Markhard AL, Nada S, Sabatini DM. Ragulator-Rag complex targets mTORC1 to the lysosomal surface and is necessary for its activation by amino acids. Cell. 2010; 141:290–303. [PubMed: 20381137]
34. Dutta S, Baehrecke EH. Warts is required for PI3K-regulated growth arrest, autophagy, and autophagic cell death in Drosophila. Curr Biol. 2008; 18:1466–75. [PubMed: 18818081]

35. Guo JY, Chen HY, Mathew R, Fan J, Strohecker AM, Karsli-Uzunbas G, et al. Activated Ras requires autophagy to maintain oxidative metabolism and tumorigenesis. Genes Dev. 2011; 25:460–70. [PubMed: 21317241]

36. Huang J, Wu S, Barrera J, Matthews K, Pan D. The Hippo signaling pathway coordinately regulates cell proliferation and apoptosis by inactivating Yorkie, the Drosophila Homolog of YAP. Cell. 2005; 122:421–34. [PubMed: 16096061]

37. Chen CL, Schroeder MC, Kango-Singh M, Tao C, Halder G. Tumor suppression by cell competition through regulation of the Hippo pathway. Proc Natl Acad Sci U S A. 2012; 109:484–9. [PubMed: 22190496]

38. Chang YY, Neufeld TP. An Atg1/Atg13 complex with multiple roles in TOR-mediated autophagy regulation. Mol Biol Cell. 2009; 20:2004–14. [PubMed: 19225150]

39. Brand AH, Perrimon N. Targeted gene expression as a means of altering cell fates and generating dominant phenotypes. Development. 1993; 118:401–15. [PubMed: 8223268]

40. Lee T, Luo L. Mosaic analysis with a repressible cell marker (MARCM) for Drosophila neural development. Trends Neurosci. 2001; 24:251–4. [PubMed: 11311363]

41. Pircs K, Nagy P, Varga A, Venkei Z, Erdi B, Hegedus K, et al. Advantages and Limitations of Different p62-Based Assays for Estimating Autophagic Activity in Drosophila. PLoS ONE. 2012; 7:e44214. [PubMed: 22952930]

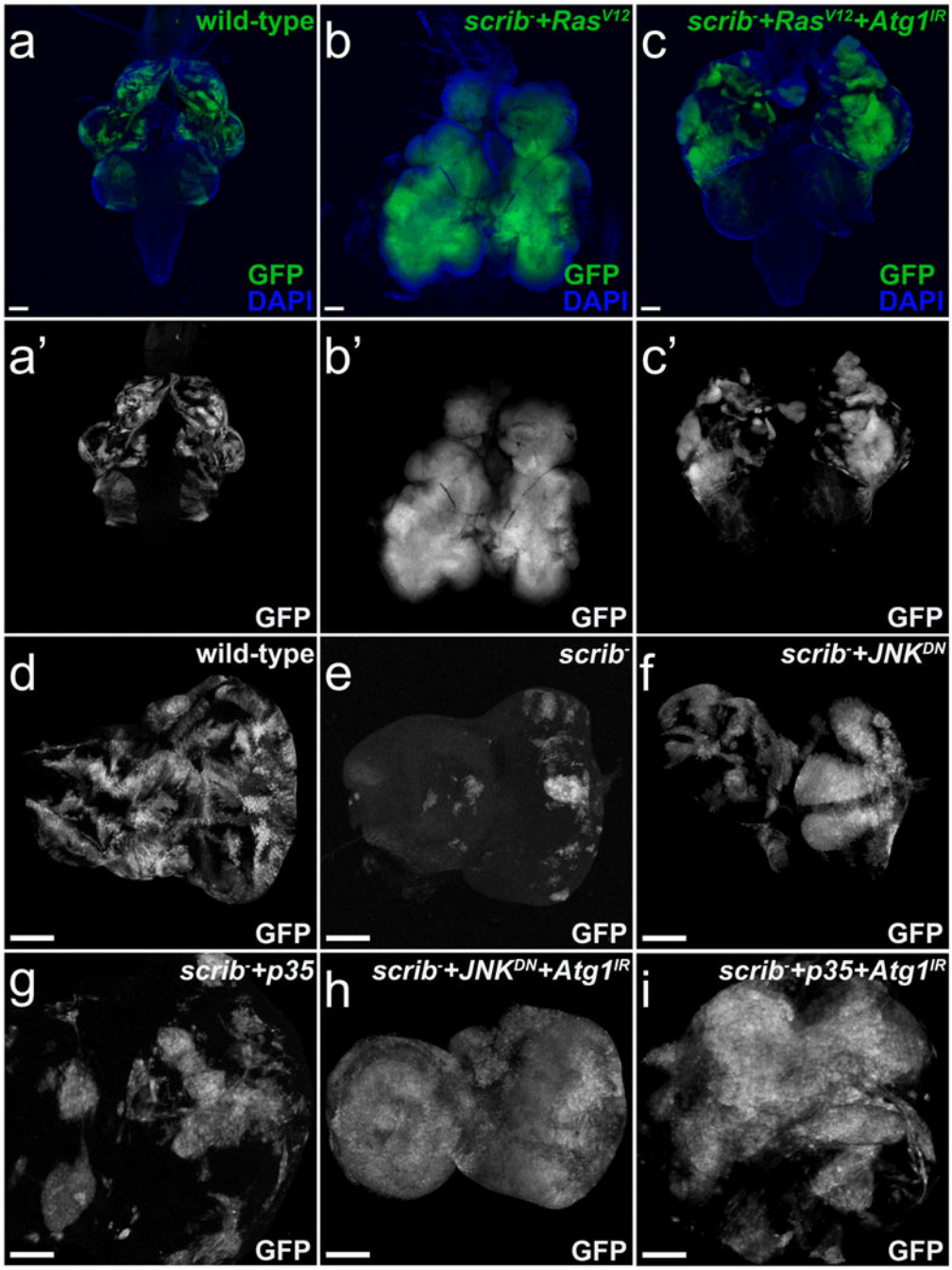

Figure 1.

Activated Ras status impacts the influence of autophagy on growth. Wild-type control clones (**a,a′,d**), *scrib* clones (**e**) and *scrib* mutant clones expressing various transgenes (**b,b′,c,c′,f,g,h,i**) were induced by MARCM and are labeled by GFP (green in a-c, grey in a′-c′,d-i). (**a-c′**) Tissue complexes of mosaic eye-antennal imaginal discs and optic lobes of wild-type (**a**), *scrib+Ras*^{V12} (**b**) and *scrib+Ras*^{V12}*+Atg1*^{IR} (**c**) 3rd instar larvae labeled for GFP and DAPI (green and blue in **a-c**) or just GFP (grey in **a′-c′**). DAPI (blue) marks the outline of the tissue. Expression of *Ras*^{V12} dramatically increases *scrib* clone size (compare **a′ and**

b′). The eye-antennal imaginal discs are strongly overgrown and absorb the optic lobe such that both tissues cannot be separated (**b**). RNAi targeting *Atg1* strongly reduces *scrib +Ras^{V12}* clone size (**c′**). The outline of the optic lobe is visible (**c**). (**d-g**) Mosaic eye antennal imaginal discs of wild-type (**d**) *scrib* (**e**) *scrib+JNK^{DN}* (**f**) and *scrib+p35* (**g**) 3rd instar larvae labeled for GFP (grey). Expression of either dominant negative JNK (*JNK^{DN}*) or the caspase inhibitor p35 strongly increases *scrib* cell clone size (**f,g**) compared to wild-type (**d**). (**h-i**) Mosaic eye antennal imaginal discs of *scrib+JNK^{DN}+Atg1^{IR}* (**h**) and *scrib +p35+Atg1^{IR}* (**i**) 3rd instar larvae labeled for GFP (grey). Decreased Atg1 function increases *scrib* clone size even more (**h,i** compared to **f**,**g**). IR – inverted repeats. Scale bars, 100 μm. Genotypes: (**a,a′**) yw *ey-FLP/+*; *Act>y^{+}>gal4, UAS-GFP^{56ST}/+*; *FRT82B tub-Gal80/ FRT82B w^{+}*. (**b,b′**) *yw ey-FLP/+*; *Act>y^{+}>gal4, UAS-GFP^{56ST}/+*; *FRT82B tub-Gal80/ Ras^{V12}FRT82B scrib^{2}*. (**c,c′**) *yw ey-FLP/+*; *Act>y^{+}>gal4, UAS-GFP^{56ST}/UAS-Atg1^{IR}; FRT82B tub-Gal80/UAS-Ras^{V12}FRT82B scrib^{2}*. (**d**) *yw ey-FLP/+*; *Act>y^{+}>gal4, UAS-GFP^{56ST}/+*; *FRT82B tub-Gal80/FRT82B w^{+}*. (**e**) *yw ey-FLP/+*; *Act>y^{+}>gal4, UAS-GFP^{56ST}/sp or Cyo; FRT82B tub-Gal80/FRT82B scrib^{2}*. (**f**) *yw ey-FLP/UAS-bsk^{DN}; Act>y^{+}>gal4, UAS-GFP^{56ST}/sp or Cyo; FRT82B tub-Gal80/FRT82B scrib^{2}*. (**g**) *yw ey-FLP/+*; *Act>y^{+}>gal4, UAS-GFP^{56ST}/UAS-p35; FRT82B tub-Gal80/FRT82B scrib^{2}*. (**h**) *yw ey-FLP/UAS-bsk^{DN}; Act>y^{+}>gal4, UAS-GFP^{56ST}/UAS-Atg1^{IR}; FRT82B tub-Gal80/FRT82B scrib^{2}*. (**i**) *yw ey-FLP/+*; *Act>y^{+}>gal4, UAS-GFP^{56ST}/UAS-Atg1^{IR}, UAS-p35; FRT82B tub-Gal80/FRT82B scrib^{2}*.

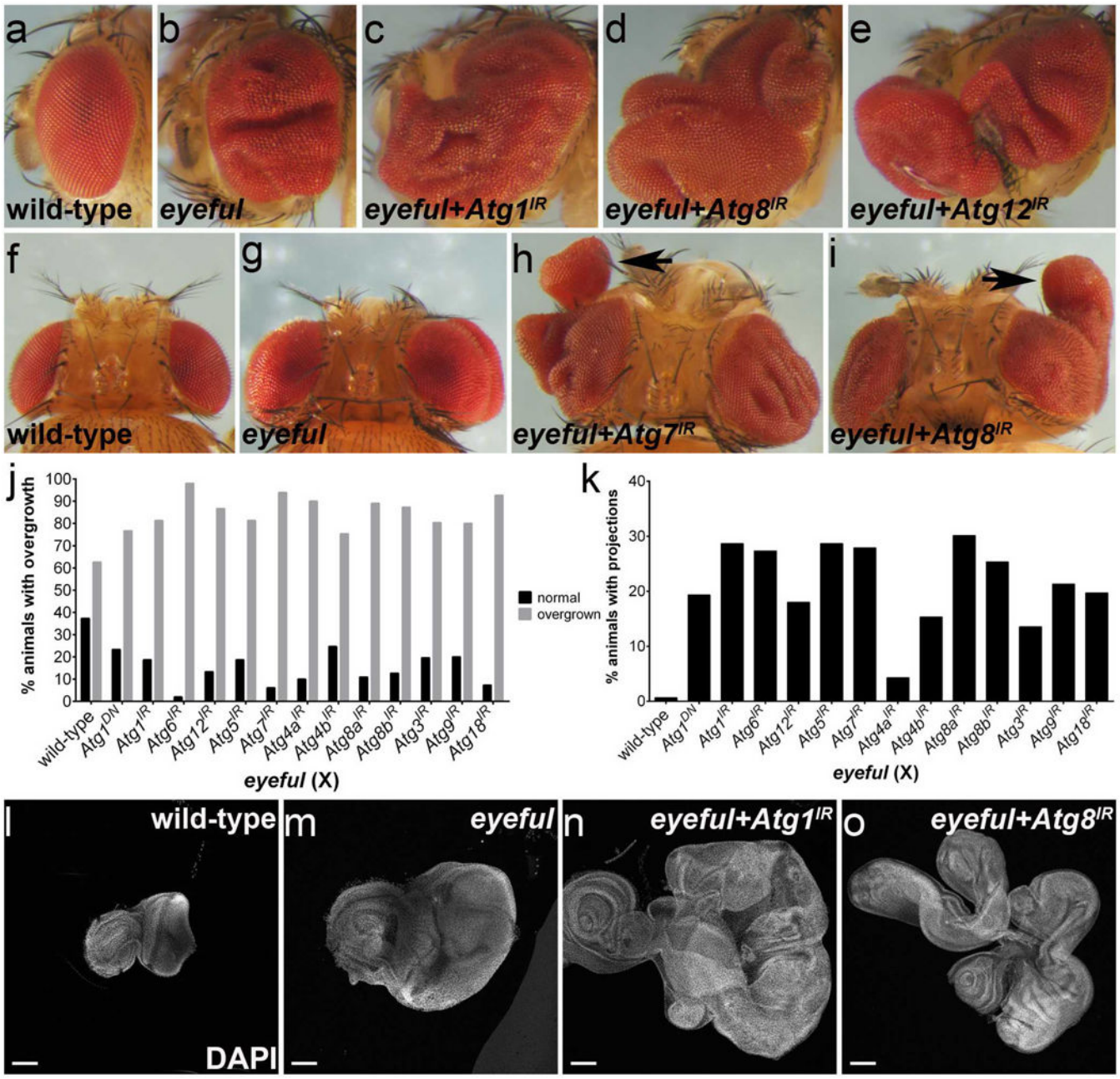

Figure 2.

Endogenous autophagy restricts *eyeful*-induced tissue overgrowth. (**a-e**) Side view images of adult eyes. (**a**) Wild-type. (**b**) *eyeful*. (**c-e**) Expression of UAS-based RNAi transgenes targeting *Atg1*, *Atg8*, or *Atg12* enhances *eyeful* induced overgrowth. (**f-i**) Top views of adult heads. (**f**) Wild-type. (**g**) *eyeful*. (**h,i**) Expression of UAS-based RNAi transgenes targeting *Atg7* (**h**) and *Atg8* (**i**) strongly enhances *eyeful*-induced overgrowth and also triggers eye tissue outgrowth in the form of projections (arrows). (**j**) Quantification of animals with overgrown adult eyes. Expression of transgenes encoding a dominant negative *Atg1* (*Atg1*^{DN}) and RNAi constructs targeting *Atg1*, *Atg6*, *Atg12*, *Atg5*, *Atg7*, *Atg4*, *Atg8*, *Atg3*,

Atg9, and Atg18 increases the percentage of *eyeful* animals with overgrown eyes. Overgrown eyes include eyes with tissue folds, eye projections and secondary eye growths. (**k**) Quantification of animals with eye projections only. Expression of transgenes encoding a dominant negative *Atg1* (*Atg1^{DN}*) and RNAi constructs targeting *Atg1, Atg6, Atg12, Atg5, Atg7, Atg4, Atg8, Atg3, Atg9, and Atg18* increases the percentage of *eyeful* animals with eye projections. (**l-o**) 3rd instar larval eye-antennal imaginal discs stained with DAPI to reveal disc outline. Scale bars, 100 μm. (**l**) wild-type. (**m**) *eyeful*. (**n,o**) Knockdown of *Atg1* and *Atg8* enhances *eyeful*-induced overgrowth. Genotypes: (**a,f,l**) CantonS; (**b,g,m**) *eyeful/+*; (**c**) *eyeful/UAS-Atg1^{IR}*; (**d,i,o**) *eyeful/UAS-Atg8^{IR}*; (**e**) *eyeful/UAS-Atg12^{IR}*; (**h**) *eyeful/UAS-Atg7^{IR}*; (**n**) *eyeful/UAS-Atg1^{IR}*. The graphs in (**j**) and (**k**) express the indicated transgenes in an *eyeful* background. 150 flies per genotype were counted. IR – inverted repeats.

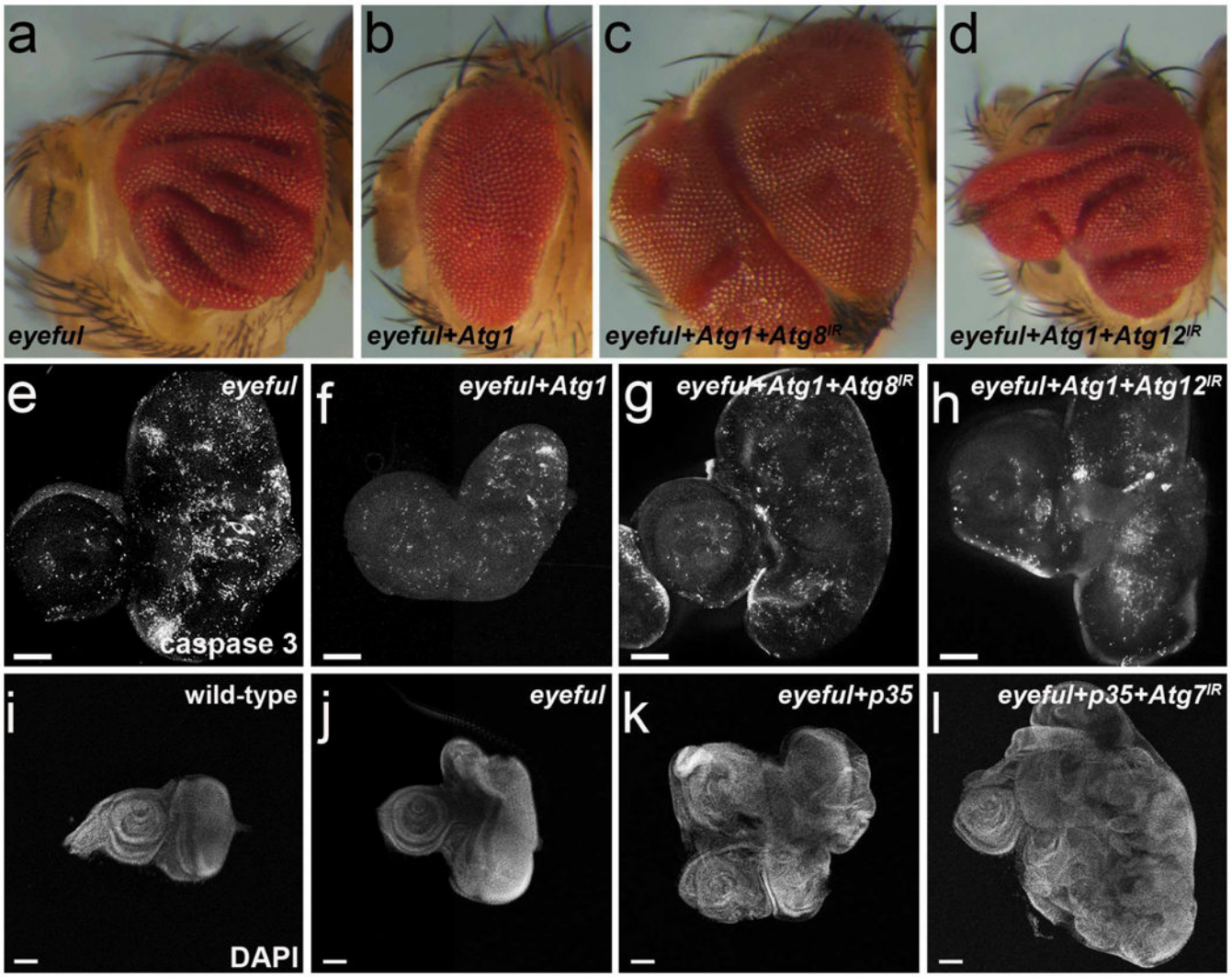

Figure 3.

Suppression of *eyeful* overgrowth by *Atg1* expression is dependent on autophagy. (**a-d**) Side view images of adult eyes. (**a**) *eyeful*. (**b**) Expression of *Atg1* suppresses *eyeful*-induced overgrowth. (**c,d**) Expression of RNAi transgenes targeting *Atg8* and *Atg12* reverses the suppression of *eyeful* induced overgrowth by *Atg1*. Eye tissue is overgrown compared to (**a,b**). IR – inverted repeats. (**e-h**) 3rd instar larval eye-antennal imaginal discs labeled for cleaved caspase-3 (cCas3) to detect apoptotic cells. (**e**) cCas3 labeling of *eyeful* discs. (**f**) cCas3 labeling of *eyeful* discs expressing *Atg1*. (**g,h**) cCas3 labeling of *eyeful* discs co-expressing *Atg1* and RNAi transgenes targeting *Atg8* or *Atg12*. (**i-l**) 3rd instar larval eye-antennal imaginal discs labeled with DAPI to outline discs. (**i**) Wild-type; (**j**) *eyeful*. (**k**) Expression of *p35* in *eyeful* animals enhances overgrowth. (**l**) Expression of *p35* and RNAi transgene targeting *Atg7* further enhances overgrowth. Scale bars, 100 μm. Genotypes: (**a,e**) *eyeful/+*. (**b,f**) *eyeful/+*; *UAS-Atg1* ^{GS10797}/+. (**c,g**) *eyeful/CyO; UAS-Atg8*^{IR}, *UAS-Atg1* ^{GS10797}/+. (**d,h**) *eyeful/UAS-Atg12*^{IR}, *UAS-Atg1* ^{GS10797}/+. (**i**) CantonS. (**j**) *eyeful/+*. (**k**) *eyeful/UAS-p35*. (**l**) *eyeful/UAS-p35; UAS-Atg7*^{IR}/+.

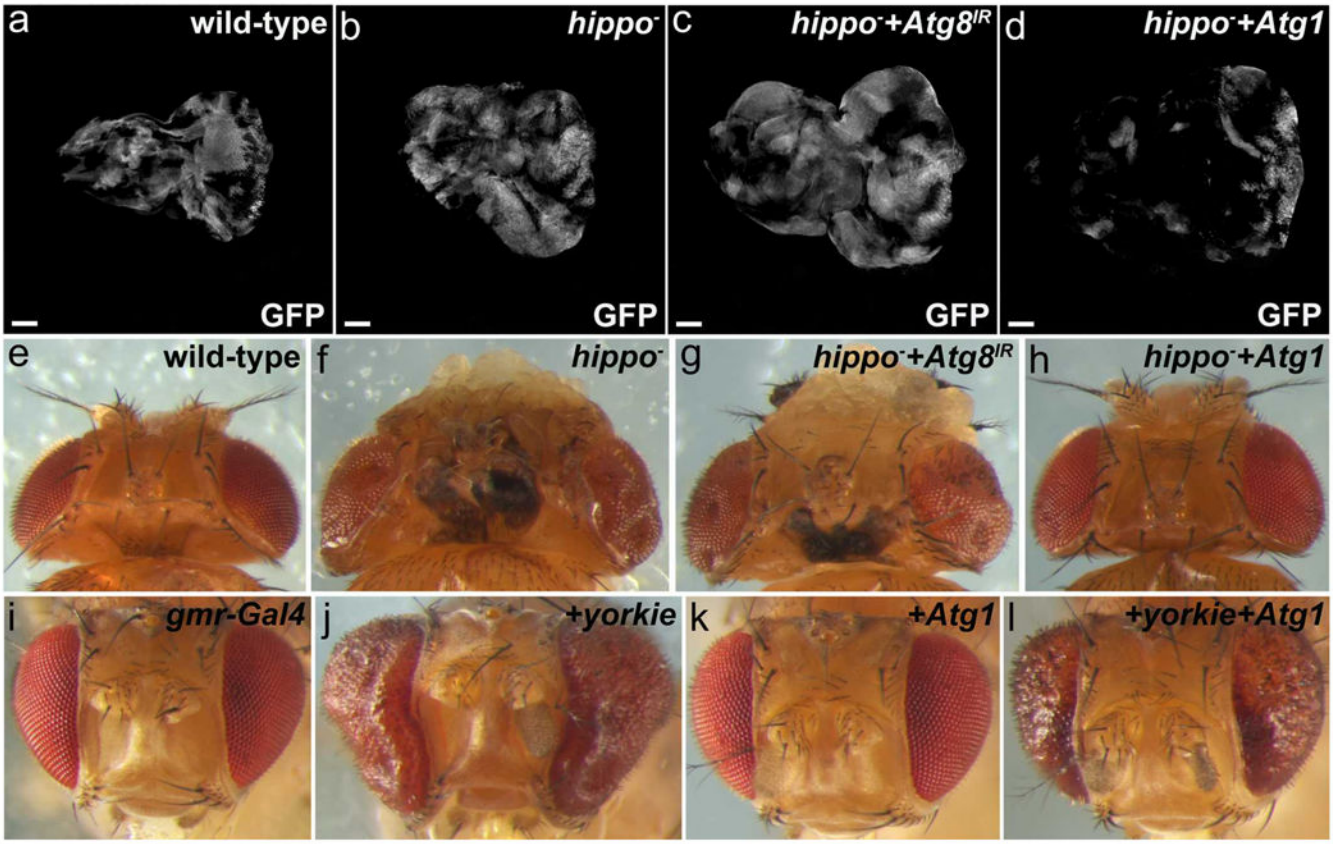

Figure 4.

While endogenous autophagy has no effect on *hippo*$^{-}$ induced tissue overgrowth, induction of autophagy suppresses it. (**a-d**) Prepupal eye imaginal discs stained with DAPI to outline disc size and morphology. GFP depicts control and *hippo* clones induced by MARCM. Posterior is to the right. (**a**) Wild-type (control) MARCM mosaic. (**b**) *hippo* mutant clones and overall eye discs are overgrown. (**c**) Expression of *Atg8* RNAi in *hippo*$^{-}$ clones does not significantly affect clone size. (**d**) Expression of *Atg1* in *hippo*$^{-}$ clones strongly reduces clone size. (**e**) Top view of wild-type MARCM adult mosaic showing eyes and head capsule. (**f**) Eyes and head capsule are overgrown in *hippo*$^{-}$ mosaic adults. (**g**) Expression of *Atg8* RNAi in *hippo* mutant clones does not suppress overgrowth of eyes and head capsule in *hippo*$^{-}$ mosaic adults (compare to **f**). (**h**) Expression of *Atg1* in *hippo*$^{-}$ clones suppresses overgrowth of eyes and head capsule of *hippo* mosaics (compare to **f**). (**i-l**) Shown are adult eyes which express the indicated transgenes using *gmr-Gal4*. Crosses were kept at room temperature (22°C). (**i**) Wild-type. (**j**) Expression of *yorkie* induces overgrowth of eyes (compare to **i**). (**k**) Expression of *Atg1*. (**l**) Expression of *Atg1* suppresses *yorkie* induced overgrowth of eyes (compare to **j**). Scale bars, 100 μm. Genotypes: (**a,e**) *yw ey-FLP/+; FRT42D tub-Gal80/FRT42D yw*$^{+}$*; tub-Gal4 UAS-CD8-GFP/+*. (**b,f**) *yw ey-FLP/+; FRT42D tub-Gal80/FRT42D hippo*^{3D}*; tub-Gal4 UAS-CD8-GFP/+*. (**c,g**) *yw ey-FLP/+; FRT42D tub-Gal80/FRT42D hippo*^{3D}*; tub-Gal4 UAS-CD8-GFP/UAS-Atg8*^{IR}. (**d,h**) *yw ey-FLP/+; FRT42D tub-Gal80/FRT42D hippo*^{3D}*; tub-Gal4 UAS-CD8-GFP/UAS-Atg1*^{GS10797}. (**i**) *gmr-*

Gal4/+. (**j**) *gmr-Gal4/+*; *UAS-yorkie/+*. (**k**) *gmr-Gal4/+*; *UAS-Atg1*^{GS10797}*/+*. (**l**) *gmr-Gal4/+*; *UAS-yorkie/ UAS-Atg1*^{GS10797}.

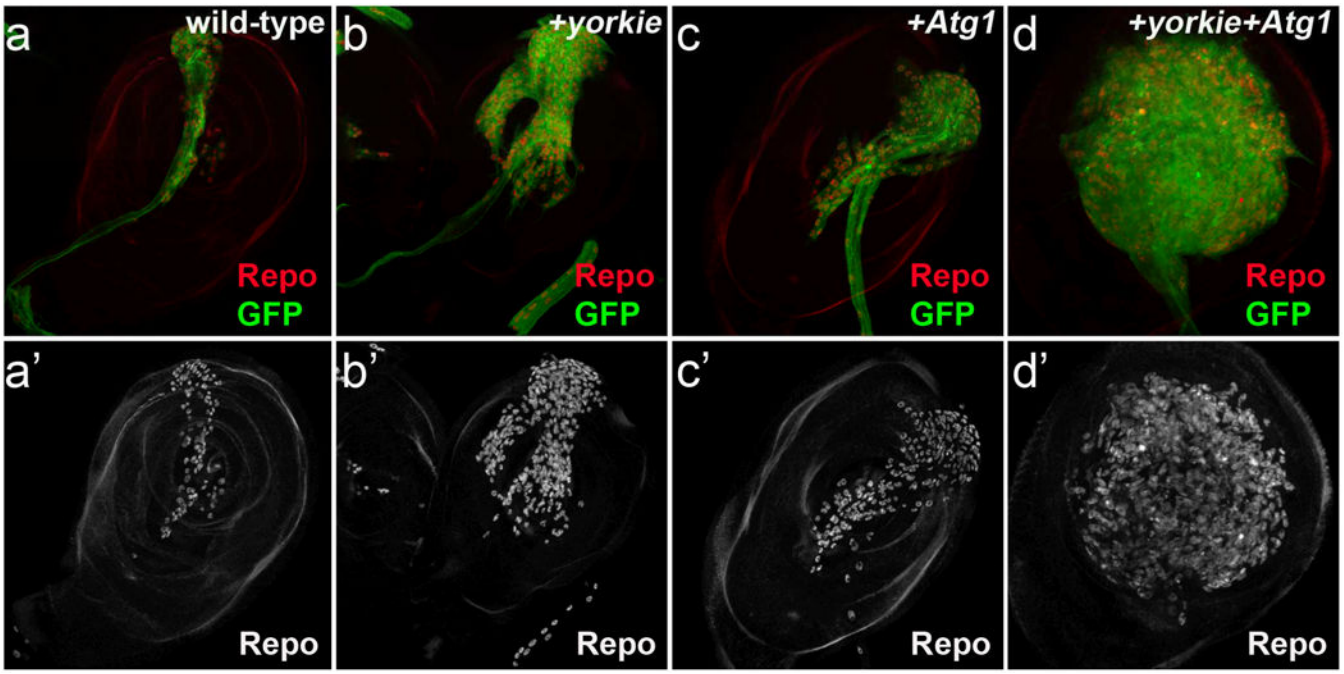

Figure 5.

Induction of autophagy enhances *yorkie*-induced overgrowth in glia cells. Shown are 3rd instar larval leg imaginal discs which express the indicated transgenes using *repo-Gal4*. Anti-Repo antibody (red) and GFP (green) labels glia cells in (**a-d**), anti-repo labelings alone in (**a′-d′**) is in grey. (**a,a′**) Wild-type. (**b,b′**) Expression of *yorkie* increases the number of glia (**b,b′**) compared to control (**a,a′**). (**c,c′**) Expression of *Atg1* slightly increases the number of glia (**c,c′**) compared to control (**a,a′**). (**d,d′**) Simultaneous expression of *yorkie* and *Atg1* dramatically increases the number of glia (**d,d′**) compared to *yorkie* (**b,b′**) or *Atg1* (**c,c′**) expression alone. Genotypes: (**a**) *UAS-dicer2/+; repo-Gal4, UAS-MCD8::GFP/+*. (**b**) *UAS-dicer2/+; repo-Gal4, UAS-MCD8::GFP/UAS-yorkie*. (**c**) *UAS-dicer2/+; repo-Gal4, UAS-MCD8::GFP/UAS-atg1*^{GS10797}. (**d**) *UAS-dicer2/Sco* or *CyO; repo-Gal4, UAS-MCD8::GFP/UAS-yorkie, UAS-Atg1*^{GS10797}.